

Research Article

Natural Fibre-Reinforced Biofoams

Anne Bergeret and Jean Charles Benezet

Centre des Matériaux de Grande Diffusion, Ecole des Mines d'Alès, 6 avenue de Clavières, 30319 Alès, France

Correspondence should be addressed to Anne Bergeret, anne.bergeret@mines-ales.fr

Received 8 April 2011; Accepted 24 June 2011

Academic Editor: James Njuguna

Copyright © 2011 A. Bergeret and J. C. Benezet. This is an open access article distributed under the Creative Commons Attribution License, which permits unrestricted use, distribution, and reproduction in any medium, provided the original work is properly cited.

Starches and polylactic acids (PLAs) represent the main biobased and biodegradable polymers with potential industrial availability in the next decades for “bio” foams applications. This paper investigates the improvement of their morphology and properties through processing and materials parameters. Starch foams were obtained by melt extrusion in which water is used as blowing agent. The incorporation of natural fibres (hemp, cellulose, cotton linter, sugarcane, coconut) in the starch foam induced a density reduction up to 33%, a decrease in water absorption, and an increase in mechanical properties according to the fibre content and nature. PLA foams were obtained through single-screw extrusion using of a chemical blowing agent that decomposed at the PLA melting temperature. A void content of 48% for PLA and 25% for cellulose fibre-reinforced PLA foams and an improvement in mechanical properties were achieved. The influence of a fibre surface treatment was investigated for both foams.

1. Introduction

Global warming, growing awareness in environmental and waste management issues, dwindling fossil resources, and rising oil prices are some of the reasons why lightweight “bio” products such as “bio” foams are increasingly promoted regarding sustainable development in material applications.

In this context, “bio” foams based on starches and biopolyesters such as polylactic acids (PLAs) have a great industrial potential, since starch foams can be considered as good candidates to substitute expanded polystyrene used for food trays in packaging industries. Moreover, PLA foams are promising alternatives to polyolefin-based foams for many automotive parts. They could be also used as efficient carriers for active pharmaceutical ingredients allowing drug release to be controlled and bioavailability to be enhanced.

Starches and PLA can be associated to biodegradable fillers leading to commonly named “bio” composites.

The poor mechanical properties of starchy materials compared to conventional oil-based polymers can be improved by adding natural fibres. Starches have been yet associated to numerous fibres among which jute fibres [1], ramie fibres [2], flax fibres [1, 2], tunicin, whiskers [3], bleached leafwood fibres [4], wood pulp [5] or microfibrils from potato pulp [6]. Most of these studies showed a high

compatibility between starch and natural fibres leading to higher stiffness. A reduction in water absorption was also obtained thanks to the higher hydrophobicity of natural fibres which was linked to the high crystallinity of cellulose. The improvement of the properties of natural fibre reinforced starch biocomposites foams was ascribed to the formation of a tight three-dimensional network between carbohydrates through hydrogen bonds.

PLA was also associated to kenaf fibres [7], jute fibres [8], flax fibres [9], rice, and wheat husks [10]. Much literature was focused on fibre surface treatments able to improve fibre/PLA interactions, among them physical (corona [11], cold plasma [12], mercerization [13]...) and chemical treatments (silane agents [14], isocyanates [15]...).

This paper exposes investigations carried out on natural fibre reinforced starch and PLA foams. The relationships existing between the material formulations, the processing conditions, the cellular morphology, and the final biocomposites foams properties, especially the mechanical properties, were highlighted in this paper.

2. General Aspects on Polymer Foams

Polymer foams are made of a solid and a gas phase mixed together upon processing. Foams with air bubbles or cells

being either closed-cells or open-cells are obtained, open-cell foams being usually more flexible than closed-cell foams. The gas used as blowing agent is either a chemical or a physical blowing component. Chemical blowing agents react in the extruder to give off the foaming gas, mainly through thermally induced decomposition reactions. Physical blowing agents are gases that do not chemically react during the foaming process and are therefore inert towards the polymer matrix.

In this study, starch foams are obtained by melt extrusion in which water is used as blowing agent as it turns into steam under temperature and pressure conditions of the extrusion. To enhance the number of cells and to homogenise the cellular microstructure, additives such as nucleating agents, that is, talc, are used. PLA foams are obtained by melt extrusion using a chemical blowing agent (called CBA) which decomposes at the PLA melting temperature.

The foaming capacity of the polymer materials was assessed by the measurement of the void content of the final product after extrusion. The experimental results allow defining an optimum set of extrusion conditions (screw profile and speed, cooling temperature, extrusion temperatures along the screw...) and material formulations (CBA content, fibre content and nature...) to improve void content and foams properties. The cell morphology (number, dimensions, shape...) and the mechanical properties (tensile, bending...) are analyzed.

3. Natural Fibre-Reinforced Starch Foams

3.1. Materials and Processing Equipments. Potato starch from Roquette Co. (France) (10–25 wt% amylose, 75–80 wt% amylopectin, 0.05 wt% proteins based on dry weight) was used for this study. Starch was mixed with different natural fibres, such as cotton linter fibres, hemp fibres, cellulose fibres, sugarcane fibres, and coconut fibres. Table 1 summarizes natural fibres main characteristics. Sugarcane and coconut fibres were submitted to specific a surface treatment described in Section 3.4.

A single-screw extruder (FairEx, 720 mm length, 30 mm diameter, 1.5×40 mm flat die, 2.31 compression rate) with 6 heating zones and a corotating twin-screw extruder (Clextral BC21, 900 mm length, 25 mm diameter, 1.5×40 mm² flat die) with 12 heating zones extruder were used for foams extrusion. Water was added with a peristaltic pump and sheet-shaped samples were obtained by calendaring of the extruded foams. Three fibre contents were compared: 7, 10, and 15 wt%. Regular expansion was achieved by adding 2 wt% of talc (Rio Tinto Minerals, France) and 2 wt% of CBA (Hydrocerol ESC5313 supplied by Clariant Masterbatches Co, France).

3.2. Determination of an Optimum Set of Extrusion Conditions. Most of the formulations were produced through twin-screw extrusion, except one which was produced through single-screw extrusion which is the industrial processing commonly used for food packaging.

3.2.1. Twin Screw Extrusion. The following processing parameters were optimized for twin-screw extrusion: screw profile, screw speed, temperature profile, mass flow rate, and water content. Restrictive elements (such as reverse pitch screws) in corotating twin-screw extrusion increase the local pressure along the barrel which favour the polymer transport as well as the expansion at the extruder die. Using screw profile 1 (see Table 2) at 200 rpm with a temperature profile from 30 to 120°C from input to die, pressure was increasing too quickly and the torque exceeded its maximum working point (110 Nm) so that the material could not be conveyed through the extruder. As a consequence, the best set of extrusion conditions was obtained without restrictive elements and a full conveying system (profile 2) (Table 3). Screw rotation speed must be high enough to reduce the residence time in the extruder but at the same time, this one must not increase shear rate within the extruder. The influence of screw speed was studied in the range of 190–430 rpm, and the optimum was found at 300 rpm. In this case, several die temperatures (from 100 to 180°C) were compared for a given screw speed of 200 rpm. It was observed that no expansion occurred for a die temperature below 100°C and a maximum expansion for 160°C. Table 4 describes the optimum temperature profile along the 12 heating zones of the extruder.

A low polymer flow (2 kg/h) should be used to avoid starch degradation. Water acts as a foaming agent as well as a plasticizer. The water content must be carefully adjusted. This optimization is difficult because starch inherently contains some water that can vary according to the storage conditions (residence time, relative humidity). It is commonly known [16] that water content ranged between 15 and 30%. Based on the twin-screw and temperature profiles defined on Tables 3 and 4, respectively, an optimized value of 17% of water gave the best expansion. In these conditions, all formulations were processed with specific mechanical energy (SME) values between 60 and 90 W·h/kg.

3.2.2. Single Screw Extrusion. For single-screw extrusion, only two processing parameters need to be studied: screw rotation speed and barrel temperature profile. Screw rotation speeds ranging from 10 to 120 rpm were compared, with the best expansion being obtained at 50 rpm corresponding to a torque between 30 and 40 Nm.

The barrel temperature profile was similar to the previous one used for the twin-screw extrusion (heating zone 1: 30°C; die: 160°C). A heterogeneous material was obtained with nonmelted granules within low expanded foam. Increasing the temperature of the feeding zone (Table 5) leads to a foam similar to the one produced by twin-screw extrusion.

3.3. Influence of the Fibre Nature and Content on the Starch Foam Characteristics

3.3.1. Density, Expansion Index, and Cell Morphology. It has to be noticed that the addition of fibres contributes to decrease the biocomposite density except for hemp fibres (Table 6). The lowest foam density was obtained with the

TABLE 1: Main characteristics of the different natural fibres used in this study.

Fibre type	Length (mm)	Cellulose content (%)	Supplier
Cotton linter	2.1	80–85	Maeda Co (Brazil)
Hemp	3.2	70–72	Chanvrière de l'Aube (France)
Cellulose	0.13	98–99	Rettenma & Söhne (Germany)
Sugarcane	12.5	80–85	Edro Ecosystems Co (Brazil)
Coconut	23.5	33	Mercedes Benz (Brazil)

TABLE 2: Twin screw profiles with two restrictive elements (noted “Rev”) (profile 1).

Screw elements	Dir	Dir	Dir	Rev	Dir	Dir	Rev
Screw thread (mm)	33	25	16.6	–33	33	16.6	–33
Screw length (mm)	325	150	50	25	100	200	50

TABLE 3: Best set of twin screw extrusion conditions with a full conveying system (profile 2).

Screw elements	Dir	Dir	Dir	Dir	Dir
Screw thread (mm)	33	25	33	25	16.6
Screw length (mm)	250	175	50	175	250

TABLE 4: Temperature profile of the twin screw extruder.

Heating zone	barrel										die	
	1	2	3	4	5	6	7	8	9	10	11	12
Temperature (°C)	30	30	50	60	70	80	90	90	100	120	120	160

TABLE 5: Temperature profile of the single screw extruder.

Heating zone	barrel					die
	1	2	3	4	5	6
Temperature (°C)	70	90	100	120	120	160

biocomposite foam reinforced by cellulose fibres. Moreover, it has been observed that the presence of fibres reduces the expansion ratio of starch foam at the exit of the die except for the biocomposite foam reinforced by cotton fibres. These contradictory effects should result from two competitive mechanisms: on one side, fibres tend to increase the viscosity of the moulded starch and, on the other side, fibres act as nucleating agents providing surfaces for cell growth. As a consequence, reinforced starch foams exhibit smaller size cells with thinner walls as shown on Table 7 and Figure 1. Results showed an open-cell structure for all formulations (about 80–82%) with low variations between them. This parameter was mainly influenced by processing conditions and especially cooling speed at the extruder die.

3.3.2. Water Absorption. Water absorption contents of the different fibres (Table 8) and of the starch-based biocomposites foams (Table 9) were measured after samples storage at various relative humidity ratios (33, 56, and 75 RH%) for 200 h. Differences of water absorption are observed between the fibres. Cotton linter fibres are less hydrophilic than hemp and cellulose fibres. These variations do not influence significantly the hydrophilicity of biocomposites foams. Indeed the presence of fibres leads to a slight decrease in starch hydrophilicity, about 1%, which does not depend

on the fibre nature [17]. This decrease could be related to the interactions between the fibres and the matrix (formation of hydrogen bonds). It can be noticed that values for starch are closed to those obtained by Soykeabkaew et al. [1].

3.3.3. Mechanical Properties. In Figure 2, bending properties (flexural modulus, maximum stress, maximum strain, modulus/density ratio, so-called specific modulus) are shown as a function of fibre nature and relative humidity (after 7 days conditioning at 33, 56, and 75 RH%) for starch foam and 10 wt% reinforced biocomposites foams.

A reinforcing effect of the fibres was observed according to the fibre nature. The best reinforcing effect was obtained with hemp fibres, followed by cellulose fibres and finally cotton linter fibres. This can be explained by the differences in fibre stiffness and length. Similar results were discussed in the literature. Several authors studied the mechanical properties of starch foams reinforced by flax, jute [1], and aspen [18, 19]. They assumed that the reinforcement effect of fibres is related to a good adhesion between fibres and matrix. In fact, starch and fibres have similar chemical structures which should favour the formation of hydrogen bonds between them. In view of the large standard deviations, it can be assumed that there are no variations of elongations at break according to the fibre nature. The values of the specific

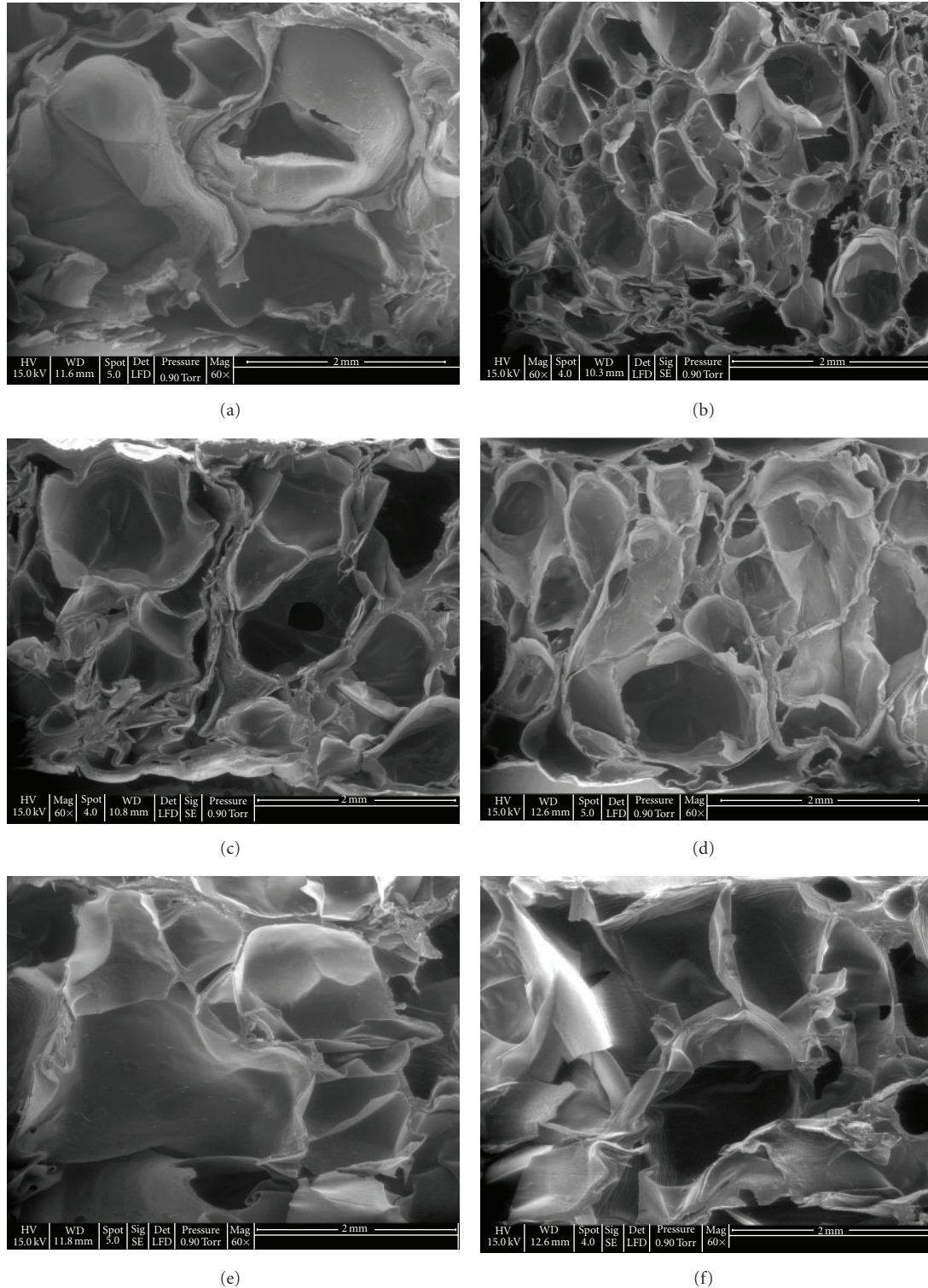


FIGURE 1: Cell morphology (a) starch foam; biocomposites foams reinforced by 10 wt% of (b) cotton linter (c) hemp and (d) cellulose fibres and 7 wt% of (e) sugarcane (f) coconut fibres.

modulus are the highest in the case of formulations with lower densities (cotton linter and cellulose fibres). According to the literature [20], this can be explained by the fact that there is no fibre orientation and that fibres are located on

the surface or in the cell-wall of the starch foam. Moreover, the reinforcing effect is decreased when relative humidity increased (from 33 to 75% RH). Lawton et al. [18] observed the same phenomenon in the case of starch foams reinforced

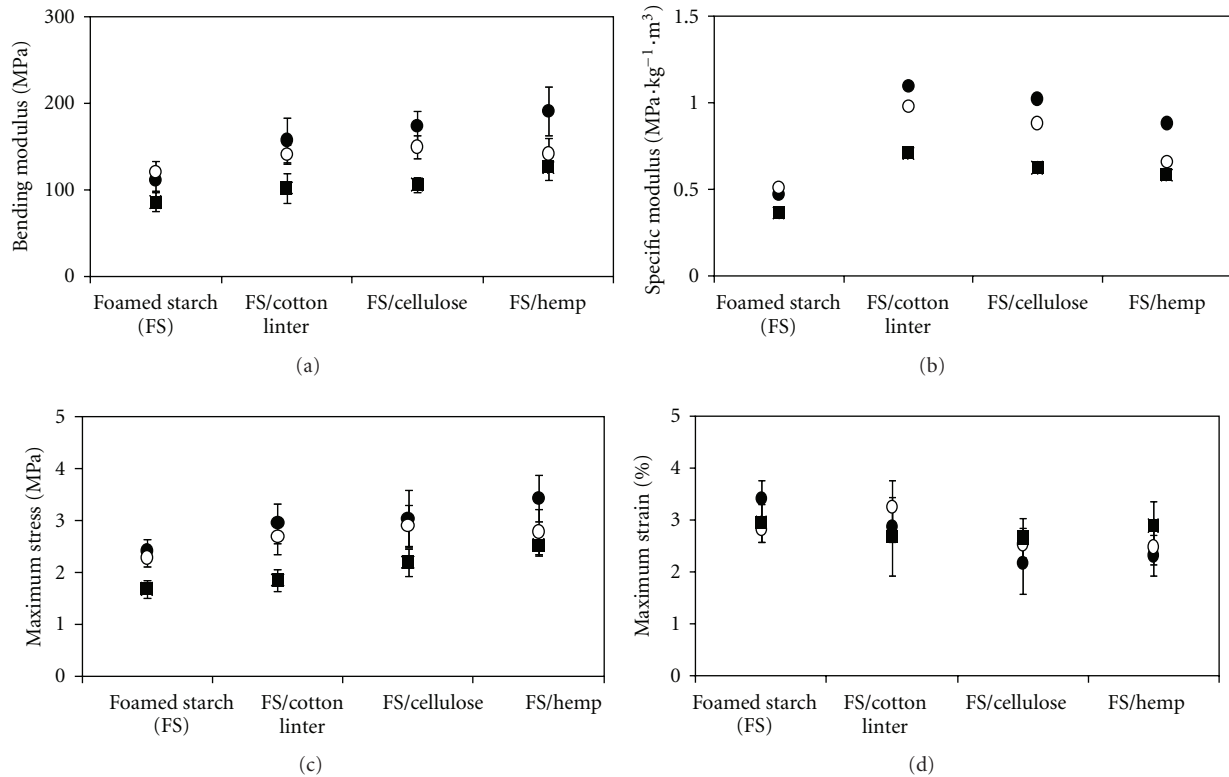


FIGURE 2: Mechanical properties of starch foam and 10 wt% reinforced biocomposites foams as a function of the fibre nature and the relative humidity: ● 33 RH%, ○ 56 RH%, ■ 75 RH%, (a) bending modulus, (b) bending modulus/density ratio, (c) maximum stress, (d) maximum strain.

TABLE 6: Densities and expansion ratios of starch-based biocomposites foams compared to starch foam.

Material	Content (wt%)	Density (g/cm ³)	Expansion ratio
Starch foam (SF)	—	0.236 ± 0.016	2.919 ± 0.213
SF/cotton linter	10	0.175 ± 0.008	3.360 ± 0.169
SF/hemp	10	0.242 ± 0.010	2.844 ± 0.171
	7	0.161 ± 0.004	2.847 ± 0.075
SF/cellulose	10	0.170 ± 0.007	2.787 ± 0.123
	15	0.158 ± 0.004	2.366 ± 0.109

with aspen fibres. It was explained by a higher plasticization of starch when relative humidity is high. The material becomes softer, and the mechanical properties decrease. Nevertheless, Soykeabkaew et al. [1] did not observe the same trends for composites reinforced by 10 wt% of jute and flax fibres. They measured an improvement of mechanical properties with increasing RH during storage from 11 to 43% and then degradation with increasing RH from 43 to 75%.

In Figure 3, bending properties are shown as a function of the cellulose fibre content and of the relative humidity (after 7 days conditioning at 33, 56, and 75 RH%). Maximum stress increases for starch foams reinforced by 7 and 10 wt% of cellulose fibres, then remained constant over 10 wt%. Results in the literature showed the same trend depending on the fibre content. Lawton et al. [18] observed an improvement in mechanical properties with fibre contents ranging from 2.5 to 15 wt%. Similarly, they

noticed a decrease in mechanical properties with increasing moisture content during storage. Regarding the evolution of the specific modulus values, an increase was observed for increasing fibre content.

3.4. Influence of the Fibre Surface Treatment. To reduce the water hydrophilicity of fibres and increase the interfacial affinity between fibres and starch foam, or change the hydrophilic/hydrophobic behavior of surfaces, some physical and/or chemical treatments are largely used. Low temperature plasma techniques were studied for polymeric surface modifications especially in presence of oxygen. Several reactors geometries have been studied to achieve the more efficient surface modification on materials.

In this part of the study, a low temperature plasma treatment was applied on sugarcane and coconut fibres

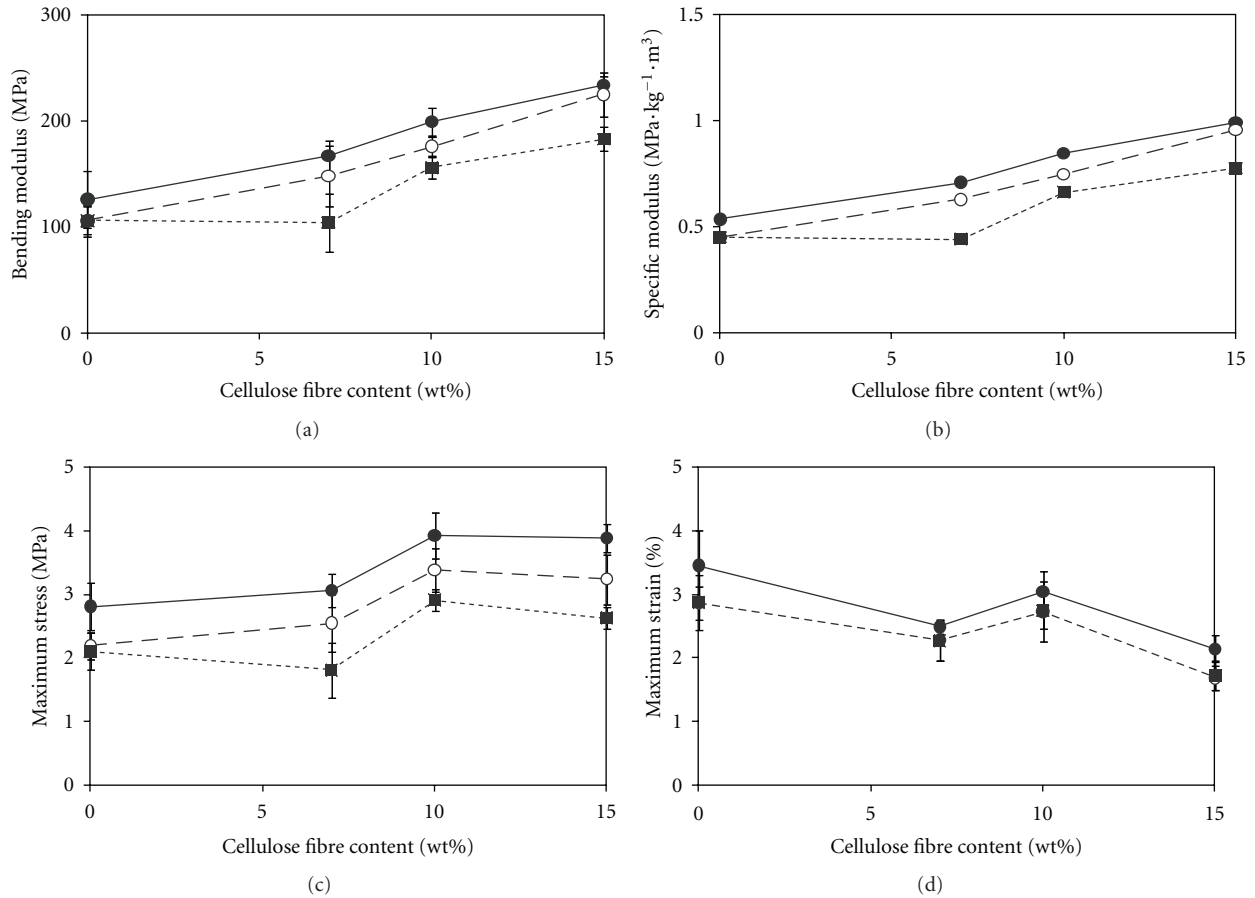


FIGURE 3: Mechanical properties of starch and biocomposites foams as a function of the cellulose fibre weight content and the relative humidity: ● 33 RH%, ○ 56 RH%, ■ 75 RH%, (a) bending modulus, (b) bending modulus/density ratio, (c) maximum stress; (d) maximum strain.

TABLE 7: Size (mean diameter in number d_n , mean diameter in weight d_w , wall thickness of cells e , polydispersity index PDI, and sphericity I_s) and open cell ratio C_o of biocomposites foams reinforced by 10 wt% of fibres compared to starch foam.

Material	d_n (μm)	d_w (μm)	PDI	e (μm)	I_s	C_o (%)
Starch foam (SF)	875.0	1046.6	0.84	21.52	0.72	80.5 \pm 0.71
SF/cotton linter	648.9	734.1	0.88	15.12	0.70	81.0 \pm 0.00
SF/hemp	784.1	966.9	0.81	17.39	0.70	82.5 \pm 0.71
SF/cellulose	577.6	730.7	0.79	12.54	0.70	82.0 \pm 0.00

(Table 1). A tubular plasma reactor was used (gas: oxygen, power: 57 W, mass treated: 15–20 g/30 min, pressure: 0.17–0.25 Pa, frequency: 13.56 MHz).

The single-screw extruder previously described was used for sample preparation. Water was added with a peristaltic pump and sheet-shaped samples were made by calendaring of the extruded foams. A fibre content of 7 wt% was tested. Regular expansion was achieved by adding 2 wt% of talc, 2 wt% of CBA, and 17 wt% of water.

Mechanical properties of biocomposites foams reinforced either by coconut or sugarcane fibres are presented on Table 10 after 6 days conditioning at 54 RH%. Foams reinforced by coconut fibres present higher mechanical properties than foams reinforced by sugarcane fibres. This

result could be explained by the difference in the initial length of these two fibres (23.5 mm against 12.5 mm). A decrease in flexural modulus is observed with plasma surface treatment whatever the fibre type but it must be noticed that standard deviations are significant. The other mechanical properties were not impacted by the treatment.

3.5. Conclusion. The physicochemical and mechanical properties were studied depending on the composition of the biocomposites foams. A decrease of the density was observed with the addition of fibres, while the expansion ratio varied depending to the fibre nature. The water absorption of the matrix was reduced by the incorporation of fibres, possibly due to the lowest hydrophilicity of fibres as compared

TABLE 8: Water absorption contents of natural fibres at various relative humidity ratios.

Material	RH (%)	Water absorption (%)
Cotton linter	33	3.78
	56	6.12
	75	9.02
Hemp	33	4.98
	56	7.84
	75	11.81
Cellulose	33	5.31
	56	7.72
	75	11.50

TABLE 9: Water absorption contents of starch-based biocomposites foams compared to starch foam.

Material	Content (wt%)	RH (%)	Water absorption (%)
Starch foam (SF)	—	33	9.10
		56	12.52
		75	16.78
SF/cotton linter	10	33	8.84
		56	11.93
		75	16.34
SF/hemp	10	33	8.75
		56	11.97
		75	16.43
SF/cellulose	7	33	9.16
		56	12.49
		75	16.72
	10	33	8.78
		56	11.51
		75	15.68
	15	33	9.11
		56	12.17
		75	15.92

to starch. The study of mechanical properties showed an improvement in the flexural behavior of biocomposites foams compared to starch foam. The highest mechanical properties were obtained with coconut fibres, and plasma treatment with oxygen did not improve their mechanical properties.

4. Natural Fibre-Reinforced Biopolyester Foams

4.1. Industrial Context. PLA is currently one of the most promising biopolymers. During the last decade, PLA has been the subject of an abundant literature with several reviews and book chapters [21–25]. Processable by many techniques (blowing films, injection moulded pieces, calendared and thermoformed films...), a wide range of PLA grades is now commercially available with companies such as Cargill (USA), Mitsui Chemical (Japan), Galactec (Belgium), Shimadzu Co (Japan), Purac (The Netherlands), and many others [26].

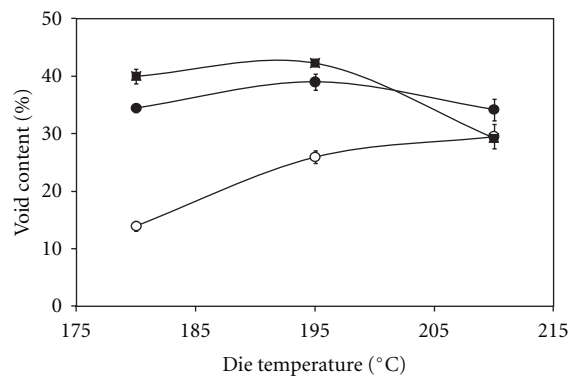


FIGURE 4: Evolution of the void content as a function of the die temperature and screw speed (●: 10 rpm, ○: 20 rpm, ■: 30 rpm) (PLA 7000D; 2 wt% CBA1; temperature profile A; free cooling).

With the aim of reducing the environmental impact of plastics, PLA-based foams products are of major industrial interest, replacing heavy items by lighter biobased products with identical performance levels. In this paper, chemically foamed structure is studied.

The objective of the studies concerned is to optimize either the processing conditions (extrusion flow rate, temperature, cooling system) or the material formulation (nature and content of chemical blowing agent, PLA characteristics) to improve foam expansion and mechanical performances. The influence of the incorporation of cellulose fibres is also studied. Different fibre aspect ratios were used, and a silane coupling agent was applied to optimize the fibre/PLA adhesion.

4.2. Determination of an Optimum Set of Extrusion Conditions. PLA 7000D (Mn = 199 600 Da, polydispersity index = 1.78 (SEC, THF, 25°C), Tg = 61°C, Tm = 153°C) provided by Nature Works LCC (USA) and Hydrocerol OMAN698483 called CBA1 (gas yield = 55 mL/g, initial and final decomposition temperatures = 160 and 220°C) provided by Clariant Masterbatches (France) were used as polymer matrix and chemical blowing agent, respectively. 2 wt% of CBA1 was incorporated in PLA.

Single-screw extrusion (FairEx, screw length = 720 mm, screw diameter = 30 mm, flat die = 40 × 1.5 mm², compression rate = 2.31) was used for foaming. Two cooling conditions, that is, a free cooling system and a confined cooling system in a three-calendaring rolls system at controlled temperature were used. Two temperature profiles (noted profile A and profile B) (Table 11) and three screw speeds ranging from 10 to 30 rpm were considered. For temperature profile A, three die temperatures were compared.

4.2.1. Influence of the Die Temperature and the Screw Rotation Speed. For a given temperature profile (profile A), results showed that the void fraction of the extruded foams reached a maximum value for an intermediate die temperature of 195°C and a screw speed of 30 rpm (Figure 4). This evolution was already reported by other authors [27, 28], and it

TABLE 10: Impact, flexural, and tensile properties for biocomposites foams (54 RH%).

Material	Impact resistance (kJ/m ²)	Flexural modulus (MPa)	Tensile strength (MPa)	Tensile elongation (%)
FS/Sugarcane	0.35 ± 0.08	98 ± 22	1.8 ± 0.4	2.9 ± 0.4
FS/treated sugarcane	0.34 ± 0.09	82 ± 22	1.9 ± 0.3	3.3 ± 1.0
FS/Coconut	0.69 ± 0.22	138 ± 70	2.8 ± 1.8	3.4 ± 1.3
FS/treated coconut	0.61 ± 0.25	110 ± 42	2.5 ± 1.1	3.3 ± 1.3

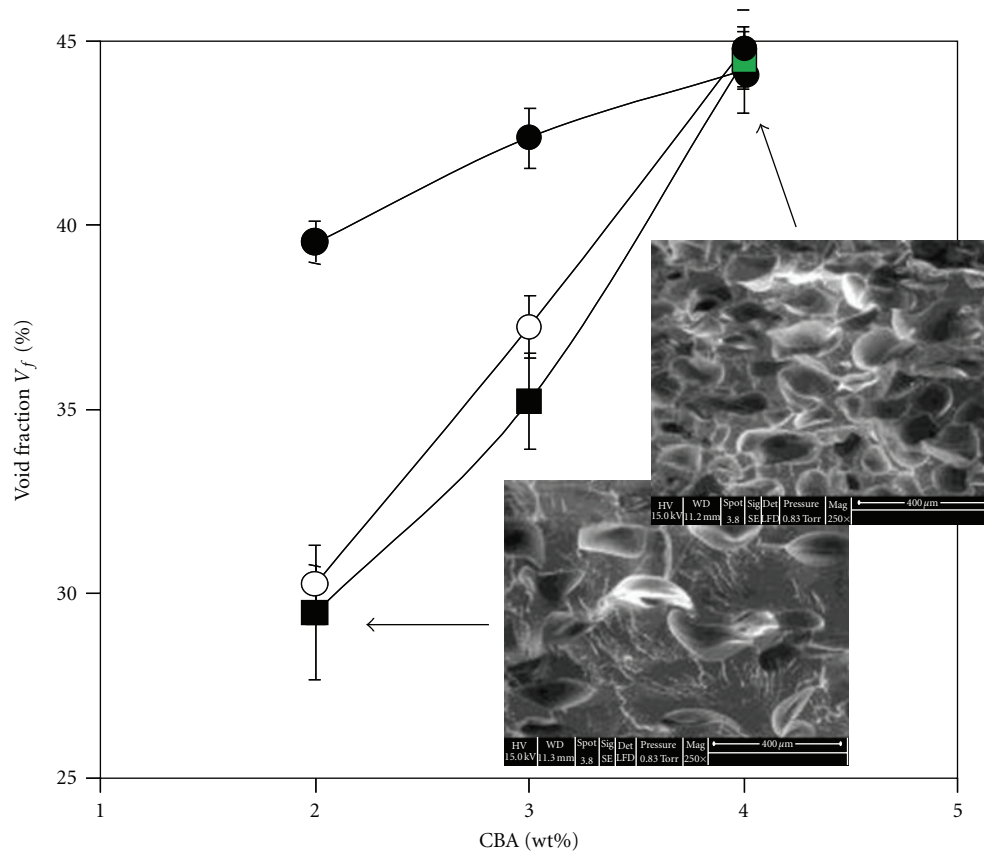


FIGURE 5: Void fraction of PLA foams as a function of the chemical blowing agent content (CBA1), the processing conditions (temperature profile: ● A; ■, ○ B) and the PLA nature (○ PLA4032D; ●, ■ PLA7000D) and corresponding microstructures (ESEM observations; magnitude 250x).

could result from a competition between two antagonist mechanisms. On one hand, an increase in temperature could favour the chemical blowing agent decomposition and thus allow the gas formation. But on the other hand, an increase in temperature could reduce the polymer viscosity and favour gas loss by diffusion through the polymer. It seems that the chemical blowing agent decomposition is predominant at low temperatures while the diffusion process is preponderant at high temperatures. Nevertheless, results obtained at the intermediate screw speed (20 rpm) are different. The void content increases with the die temperature. The simulation of the polymer flow (in particular the evaluation of temperature and viscosity distribution in the barrel and the die) are required to be able to evaluate the relative level of these two competitive mechanisms.

4.2.2. Influence of the Temperature Profile. The density and the void content of the foam extruded with the temperature

profile A were equal to 767 kg/m³ and 42%, respectively, as values of 893 kg/m³ and 33% were obtained for the foam extruded with the temperature profile B for a given die temperature (195°C) and screw rotation speed (30 rpm). It can be noticed that the temperature profile B presents higher temperatures for the first barrel zones than those of temperature profile A. Therefore, with temperature profile B, an earlier gas formation should occur (i.e., before the complete melting and the pressurization of the polymer within the barrel) leading to a significant gas loss through the hopper. The quantity of CO₂ available for the expansion process in the die should then be reduced leading to a lower void content [29].

4.2.3. Influence of the Cooling Rate. Table 12 shows that the cooling rates induced by the two cooling systems used in this study are not different enough to induce important modification of the void content and the cellular structure.

TABLE 11: Temperature profiles for PLA chemical foaming through single-screw extrusion.

Temperature profile	Temperature (°C)					Die
	Barrel (from hopper to die)					
	1	2	3	4	5	6
A	130	150	165	165	170	180-195-210
B	150	170	170	170	180	195

TABLE 12: Effect of the cooling system on the void content and the cellular structure (PLA 7000D, 2 wt% CBA1, temperature profile A, screw speed 30 rpm, die temperature 195°C)—Void content V_f , cell dimensions (d_n , d_w), cell size polydispersity (PDI), cell density (N_c), cell-wall thickness (δ)—() = standard deviation.

Cooling system	V_f (%)	\bar{d}_n (μm)	\bar{d}_w (μm)	PDI	N_c (cells/cm ³) $\times 10^4$	δ (μm)
free	47 (1)	107	122	0.88	7.38	49.26
confined	45 (1)	92	105	0.88	10.86	45.59

These results are similar to those reported by other authors [30].

4.3. Influence of the Material Formulation. PLA7000D was compared to PLA4032D ($M_n = 183\,800$ Da, polydispersity index = 1.95 (SEC, THF, 25°C), $T_g = 69^\circ\text{C}$, $T_m = 173^\circ\text{C}$) also provided by Nature Works LCC (USA). A significant difference in melting temperatures was observed between these two PLAs and was attributed to different optical purities (6.4% and 2.4% of D-lactic units for PLA 7000D and PLA 4032D, resp.).

CBA1 was compared to Hydrocerol CT3108 (gas yield = 50 mL/g, initial and final decomposition temperatures = 150 and 210°C, resp.) called CBA2 and also provided by Clariant Masterbatches (France). Each CBA was incorporated in PLA at contents varying from 2 to 4 wt%.

Single-screw processing was performed based on the optimal set of conditions previously described, that is, a screw speed of 30 rpm, a die temperature of 195°C, specific temperature profiles (A and B), and a confined cooling system.

4.3.1. Influence of the PLA Nature. The nature of PLA has no major effect on the void content of the foams extruded with a same temperature profile (B). Indeed the density varies between 894 and 879 kg/m³ corresponding to a density reduction of 33% and 34% for PLA7000D and PLA4032D, respectively, for a given content of CBA1 (2 wt%). It can be notified that the foaming of PLA4032D is not possible using the temperature profile A. The barrel temperature in the feeding and melting zones is lower than the polymer melting temperature and then not adapted for extrusion process. Nevertheless, because of the high temperatures used in the first barrel zones for temperature profile B, one can anticipate significant gas losses during extrusion. This result confirms that a compromise should be found between all processing parameters [27, 29, 31].

4.3.2. Influence of the Chemical Blowing Agent Content. Figure 5 shows that the void content increases linearly (the foam density decreases) with the CBA1 content, regardless of the PLA type or the temperature profile. This evolution is related to the amount of gas formed and available during

the expansion process [27]. Similar results were reported for extruded foams based on polyolefins [29, 32].

As shown on Table 13, the two studied PLAs provide foams with a homogeneous cellular structure (polydispersity PDI close to 1) with a relatively low open-cells ratio (between 11 and 27%). This is in agreement with results reported for polyolefin foams [27, 33, 34]. An increase in the open-cell ratio with the CBA1 content is observed which is related to the amount of gas release. This trend was already reported by other authors [27, 29]. A higher open-cell ratio range was obtained for PLA4032D (ratio between 19 and 27% for CBA1 content between 2 and 4 wt%) compared to PLA7000D (ratio between 12 and 19% for CBA1 content between 2 and 4 wt%). This is related to the higher temperatures involved in the temperature profile B used for PLA4032D compared to profile A inducing then a higher gas yielding as well as a lower PLA viscosity. According to Klemperner and Sendjarevic [27], during initial cell growing, cells are closed. As the polymer viscosity decreases, the cell-wall thickness decreases so that they should break because of an increased pressure within the cell. Regarding PLA7000D (temperature profile A), an increase in CBA1 induces an increase in the average cell diameter (about 16% for d_n). Nevertheless, the cell-wall thickness remains constant (between 46 and 49 μm). These results are related to an increase in gas volume available for cell growing and may explain the increase in void content (Figure 4). Results performed on PLA4032D are different. The variation of the average cell diameter is not linear with the CBA1 content, and larger cells are obtained for extreme CBA1 contents (2 and 4 wt%). It can be assumed that several competitive mechanisms should occur (i) the increase in gas yielding and decrease in viscosity due to the higher barrel temperatures of profile B, (ii) the plasticization induced by the gas products during decomposition, and (iii) the presence of a higher content of nucleating agents present in the CBA1 master batch. Complementary works are in progress to evaluate their relative contributions. The average cell diameter and the cell-wall thickness measured in the present study are similar to those reported for polyolefins foamed with CBA1 [27, 29], but significantly higher than those reported by other authors for microcellular PLA foams [33]. Nevertheless, the cases reported in the literature concern mainly physical foaming processes, and

TABLE 13: Cell dimensions (d_n , d_w), cell size polydispersity (PDI), cell density (N_c), cell-wall thickness (δ) as a function of the chemical blowing agent content (CBA1) (PLA 7000D temperature profile A and PLA 4032D temperature profile B; screw speed 30 rpm; die temperature 195°C; free cooling)—(): standard deviation.

PLA	CBA1 (%wt)	d_n (μm)	d_w (μm)	PDI	N_c (cells·cm ⁻³) × 10 ⁵	δ (μm)	C_o (%)
7000D	2	90	105	0.86	11.25	48.14	10.91 (0.24)
	3	95	104	0.91	10.13	46.46	14.72 (1.08)
	4	107	122	0.88	7.38	49.26	19.22 (0.69)
4032D	2	134	144	0.93	2.72	95.39	19.12 (1.47)
	3	125	174	0.72	4.02	70.80	24.49 (1.3)
	4	130	152	0.86	4.19	57.89	26.76 (1.11)

TABLE 14: PLA-foams tensile properties as a function of the chemical blowing agent content (CBA1) (PLA 7000D temperature profile A and PLA 4032D temperature profile B; screw speed 30 rpm; die temperature 195°C; free cooling)— σ_{max} : yield stress, ϵ_{max} : elongation at yield stress, σ_r : ultimate stress, ϵ_r : ultimate elongation—(): standard deviation.

PLA	CBA1 (wt%)	Void fraction (%)	σ_{max} (MPa)	ϵ_{max} (%)	σ_r (MPa)	ϵ_r (%)
7000D	0	—	60.51 (1.58)	10.33 (0.94)	57.34 (1.36)	11.12 (0.86)
	2	42 (1)	36.00 (2.84)	8.41 (0.32)	33.38 (2.18)	9.95 (0.71)
	3	45 (1)	25.65 (1.33)	8.84 (0.39)	21.51 (1.72)	11.59 (0.92)
	4	47 (1)	23.71 (0.90)	8.37 (0.55)	20.49 (1.08)	10.28 (1.16)
4032D	0	—	59.51 (2.26)	9.40 (0.42)	54.61 (4.99)	10.19 (0.61)
	2	34 (1)	40.54 (3.27)	10.24 (0.89)	37.91 (3.90)	11.51 (1.23)
	3	41 (1)	30.68 (2.40)	8.61 (0.70)	27.14 (3.44)	10.43 (1.11)
	4	48 (1)	26.77 (1.24)	9.44 (1.36)	22.87 (1.12)	11.50 (1.60)

PLA modified by nanofillers (which act as cell nucleating agents) and/or chain extenders.

Finally, for both types of PLA, the increase in CBA1 content leads to a reduction in tensile yield and ultimate stresses (Table 14), due to the increase in void content (reduction of the effective sample cross-section) and in number of cells (which act as damage initiators). On the contrary, yield and ultimate elongations are both about 10% and independent on CBA1 content. Similar results were reported in the literature for PVC and PUR-based foams [35, 36]. It is all the more interesting to evaluate the ratio tensile stress/density (so-called specific stress) to determine the efficiency of the PLA foaming. These ratios are about 46 MPa·cm⁻³·g⁻¹ for yield stress and 43 MPa·cm⁻³·g⁻¹ for ultimate stress for unfoamed PLA and for PLA foamed with 2 wt% of CBA1. Above 2 wt% of CBA1, a significant decrease in the specific stress is observed (about 34 MPa·cm⁻³·g⁻¹ for yield stress and 29 MPa·cm⁻³·g⁻¹ for ultimate stress). This behavior is independent on PLA nature.

4.3.3. Influence of the Chemical Blowing Agent Nature. PLA7000D was foamed through identical processing conditions (temperature profile A, die temperature 195°C, screw speed 30 rpm, confined cooling) with 4 wt% of CBA1 and CBA2. Similar void contents were obtained (45% for CBA1 and 43% for CBA2). The slight difference should result from small differences in gas yielding between both CBA.

Nevertheless, the cellular morphology could be different but was not evaluated here.

4.4. Influence of the Incorporation of Raw and Surface Treated Cellulose Fibres in PLA Foams

4.4.1. Fibres Characteristics and Processing. PLA7000D was reinforced by pure cellulose fibres (cellulose content = 99.5%) provided by Rettenmaier and Söhne (Germany). Four fibres (two Short Cellulose Fibres (SCF) and Cellulose MicroFibres (CMF)) were compared according to their shape factor as described in Table 15.

A silane surface treatment was applied on one of these fibres, that is, CMF1, according to an experimental procedure described by Huda et al. [37]. 5 wt% of aminopropyltriethoxysilane (APS) compared to the fibre was dissolved for hydrolysis in a mixture of water ethanol (40:60 w/w). The pH of the solution was adjusted to 4 with acetic acid and stirred continuously during 1 h. Next, the fibres were soaked in the solution for 3 h. Fibres were then washed and kept in air for 3 days. Lastly, the fibres were oven dried at 80°C for 12 h.

Bio composites (20 and 30 wt% of fibres) were compounded with a twin-screw extruder (Clextral BC21, length 900 mm, diameter 25 mm, 12 heating zones). Then, foaming

TABLE 15: Characteristics of the short cellulose fibres (SCF) and the cellulose microfibrils (CMF) used for the study.

	Length (μm)	Diameter (μm)	Shape factor	Density (g/l)	S_{BET} (m^2/g)
SCF1	130	20	6,5	155–185	0.642
SCF2	60	20	3	180–220	0.813
CMF1	40	20	2	190–250	0.780
CMF2	18	15	1,2	230–300	1.192

TABLE 16: Cell dimensions (d_n , d_w), cell density (N_c), cell size polydispersity (PDI), cell-wall thickness (δ), and open-cell ratio (C_o) as a function of the fibre nature and fibre content (PLA7000D, 3 wt% CBA2 for biocomposites foams, 4 wt% CBA2 for PLA foam, temperature profile A, screw speed 30 rpm, die temperature 195°C, free cooling)-(): standard deviation.

	Fibre (%wt)	d_n (μm)	d_w (μm)	PDI	N_c (cells·cm ⁻³) $\times 10^5$	δ (μm)	C_o (%)
7000D	0	106	131	0.81	6.98	54.74	21.68 (2.31)
SFC1	20	81	104	0.78	3.67	172.11	29.69 (0.90)
	30	59	72	0.81	—	—	30.89 (1.55)
SFC2	20	62	87	0.71	9.47	118.98	26.00 (1.39)
	30	55	70	0.79	—	—	33.25 (1.42)
CMF1	30	67	92	0.72	15.80	67.66	36.42 (2.10)
CMF2	30	79	107	0.73	6.87	109.33	38.42 (1.26)

processing was achieved with a single-screw extruder (3 wt% CFA2, temperature profile A, screw speed 30 rpm, die temperature 195°C). All results are compared to unreinforced PLA (4 wt% of CBA2).

4.4.2. Void Content and Cell Morphology. It was observed (Figure 5) that the presence of cellulose fibres induced a sharp decrease in the void content compared to unreinforced PLA7000D. It can be noticed that it was not possible to process PLA foams reinforced by 20 wt% of microfibrils because of a too low viscosity. Indeed, other investigations have shown that a drastic decrease in molecular weight occurs for these compounding samples. For 20 wt% reinforced foams, the void content is about 11% for short fibres (SFC1 and SFC2) while it is very low, for the 30 wt% reinforced foams. This could suggest that void content decreases with fibre content for PLA foaming, which is in accordance with the literature [38]. For 30 wt% microfibrils, void contents of 25 and 17% were obtained for CMF1 and CMF2, respectively. Similar results were obtained for PVC/wood flour and PP/wood flour composites [39–42].

As shown on Table 16, cell diameters decrease with the increase in fibre content whatever the shape factor of the fibres. This result could be related to an increase in the number of nucleating sites induced by the fibre surface. Cell diameters and cell densities seem to be independent of the fibre length for a given fibre weight content of 30 wt%. The cell-wall thickness is much higher for cellulose fibre reinforced PLA foams compared to unreinforced PLA foam. Moreover, the polydispersity index variations are heterogeneous in presence of fibres. These behaviors should be related to fibre distribution within PLA matrix and to the fibre/matrix interactions. Indeed, these two parameters have a direct impact on the rheological behavior and therefore on the foam morphology. Local debondings at the fibre/matrix

interface induce gas losses that will decrease the cell growing ability, and on the other hand, a heterogeneous distribution of the cell size (i.e., a low polydispersity index) is obtained when a disorganized repartition of fibres in the PLA matrix occurs. Results show also an increase in the open-cell ratio in presence of fibre compared to unreinforced PLA foam. This could be related to a low interfacial adhesion inducing microholes between fibres and polymer as suggested by other authors [39]. A linear correlation between the open-cell ratio and the developed surface of the fibres (considered as the ratio between the specific surface of the fibres determined through BET measurements and the weight content of fibres) was established.

4.4.3. Mechanical Properties. Tensile tests performed on composite foams (Table 17) do not show any significant variations according to the fibre content and length. Yield stress and strain are about 20 MPa and 7%, respectively, for all materials. Moreover, it can be observed similar specific yield and ultimate stresses (stress/density ratio) for all composites with lower values (ranging from 20 to 29 MPa·cm⁻³·g⁻¹) than those of unreinforced PLA foam (42 MPa·cm⁻³·g⁻¹). Similar data were obtained by other authors [43, 44] for PLA reinforced by hemp, microcrystalline cellulose, and wood flour. This decrease was attributed to a lack of adhesion between reinforcement systems and PLA. Nevertheless, Huda et al. [45] show inverse results for PLA reinforced by recycled cellulose fibres. These specific properties are different according to the fibre length. A slight decrease with the fibre content was observed for SFC1 as no variation can be observed for SFC2.

4.4.4. Improvement of the Interfacial Adhesion Fibre/Matrix. As shown on Figure 6, a sharp unexpected decrease in void content is obtained for CMF1_{APS} compared to CMF1. It can

TABLE 17: PLA-foams tensile properties as a function of the fibre nature, the fibre content, and the fibres surface treatment (CMF1_{APS}) (PLA7000D, 3 wt% CBA2 for biocomposites foams, 4 wt% CBA2 for PLA foam, temperature profile A, screw speed 30 rpm, die temperature 195°C, free cooling)— σ_{\max} : yield stress; ϵ_{\max} : elongation at yield stress; σ_r : ultimate stress; ϵ_r : ultimate elongation—(): standard deviation.

	Fibre (%wt)	Void fraction (%)	σ_{\max} (MPa)	ϵ_{\max} (%)	σ_r (MPa)	ϵ_r (%)
7000D	0	43 (1)	17.81 (1.41)	7.57 (0.98)	16.27 (1.33)	8.34 (1.14)
SFC1	20	10 (1)	20.12 (2.20)	7.07 (0.72)	19.89 (2.18)	7.15 (0.73)
	30	—	21.50 (1.11)	7.47 (0.33)	21.32 (1.22)	7.52 (0.33)
SFC2	20	12 (1)	23.7 (1.76)	7.30 (0.71)	23.59 (1.75)	7.34 (0.70)
	30	—	18.94 (2.59)	6.61 (0.61)	18.92 (2.58)	6.63 (0.61)
CMF1	30	25 (0)	19.69 (1.22)	6.94 (0.69)	19.55 (1.24)	6.98 (0.70)
CMF1 _{APS}	30	7 (3)	22.95 (3.33)	8.77 (0.72)	22.92 (3.32)	8.79 (0.73)
CMF2	30	17 (1)	17.91 (1.69)	7.16 (0.50)	17.84 (1.68)	7.18 (0.51)

be noticed that discrepancies exist in the literature. As an example, some authors [39] observed an increase in the void content (6 to 12% regardless to the composite) in the case of HDPE/wood flour composites. But the chemical blowing agent nature should also be considered. Besides, it could be interesting to evaluate the grafting level of silane molecules onto the cellulose fibre surface. Regarding tensile properties (Table 17), no significant improvement was observed in presence of APS surface treatment, nevertheless mean values are higher. Further investigations should be achieved to optimize the silane grafting on cellulose fibres.

4.5. Conclusion. Experimental results show that, depending on processing conditions and material formulation, a single-screw extrusion process based on chemical foaming can lead to a significant reduction in weight of unreinforced PLA foam (up to 48%) and cellulose fibre reinforced PLA foams (up to 25%) as well as an improvement in mechanical properties (tensile strength up to 30%). Nevertheless, it requires an optimized control of all process and material parameters.

5. Further Investigations

The influence of natural fibres on foaming ability needs to be clarified, as well as the influence of the fibre/matrix adhesion on the cell growing rate. For PLA-based biocomposites foams, a posterior plasma treatment could be performed to stabilize the initial plasma treatment and avoid loss of surface features. An optimization of the silane grafting conditions (preparation of polysiloxane solution, grafting duration, drying conditions...) could also be achieved. Other studies are conducted to understand the mechanisms that govern the formation of open-cells or closed-cells.

Regarding the foam properties, only mechanical properties (bending and tensile modes) were analyzed in this paper. Experiments have been achieved to study the influence of different parameters (processing and material parameters) on the biodegradation rate (mainly Biological Demand in Oxygen, BDO).

Many further investigations will be performed to understand competitive mechanisms that govern the cell formation

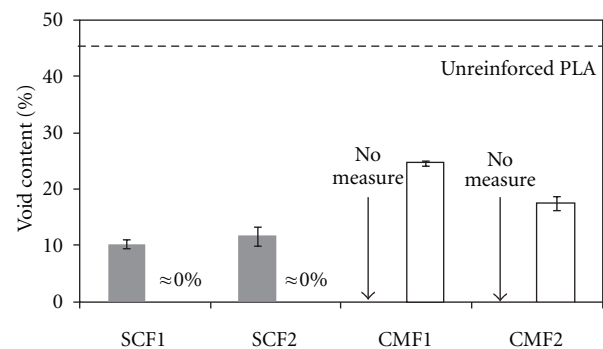


FIGURE 6: Void fraction of cellulose reinforced PLA foams as a function the fibre content: ■ 20 wt%; □ 30 wt% (PLA7000D, 3 wt% CBA2 for biocomposites foams, 4 wt% CBA2 for PLA foam, temperature profile A, screw speed 30 rpm, die temperature 195°C, free cooling).

during extrusion, especially for PLA foams, among them (i) the decrease in viscosity due to extrusion conditions that favour gas losses by diffusion through the polymer, (ii) the increase in gas yielding with increasing temperature that can induce a plasticization by the gas products, and (iii) the nucleating effects of nucleating agents and/or of natural fibres present within the polymer.

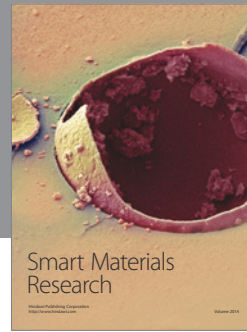
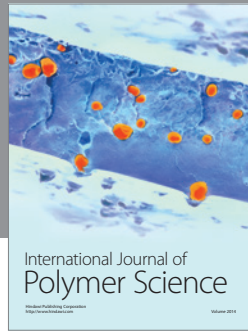
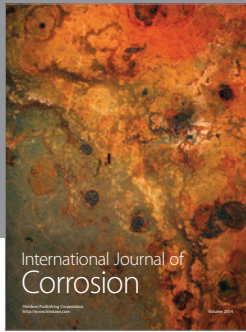
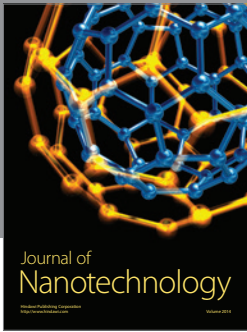
Acknowledgments

The authors are very indebted to Ph. D. students that were strongly involved in the presented studies, that is, Dr. A. Stanojlovic-Davidovic (for starch foams) and Dr. J. M. Julien (for PLA foams). Specific thanks are also devoted to Pr H. M. Viana (Centro Universitário Fundação Santo André, Santo André, SP, Brazil) for its active contribution to the study on sugarcane and coconut fibres, as well as to Pr. S. Borros (Universitat Ramon Ull, Barcelona, Spain) for the realization of the plasma treatments. Authors are also grateful to financial organization ADEME, to Vitembal Company (Remoulins, France), and to French academic institutions (Université de Toulon et du Var; Ecole des Mines de Douai).

References

- [1] N. Soykeabkaew, P. Supaphol, and R. Rujiravanit, "Preparation and characterization of jute-and flax-reinforced starch-based composite foams," *Carbohydrate Polymers*, vol. 58, no. 1, pp. 53–63, 2004.
- [2] M. Wollerdorfer and H. Bader, "Influence of natural fibres on the mechanical properties of biodegradable polymers," *Industrial Crops and Products*, vol. 8, no. 2, pp. 105–112, 1998.
- [3] M. N. Angles and A. Dufresne, "Plasticized/ tunicin whiskers nanocomposite materials. 2. Mechanical properties," *Macromolecules*, vol. 34, no. 9, pp. 2921–2931, 2001.
- [4] L. Averous, C. Fringant, and L. Moro, "Plasticized starch-cellulose interactions in polysaccharide composites," *Polymer*, vol. 42, no. 15, pp. 6571–6578, 2001.
- [5] A. J. F. de Carvalho, A. A. S. Curvelo, and J. A. M. Agnelli, "Wood pulp reinforced thermoplastic starch composites," *International Journal of Polymeric Materials*, vol. 51, no. 7, pp. 647–660, 2002.
- [6] A. Dufresne, D. Dupeyre, and M. R. Vignon, "Cellulose microfibrils from potato tuber cells: processing and characterization of starch-cellulose microfibril composites," *Journal of Applied Polymer Science*, vol. 76, no. 14, pp. 2080–2092, 2000.
- [7] T. Nishino, K. Hirao, M. Kotera, K. Nakamae, and H. Inagaki, "Kenaf reinforced biodegradable composite," *Composites Science and Technology*, vol. 63, no. 9, pp. 1281–1286, 2003.
- [8] D. Plackett, A. T. Logstrup, P. W. Batsberg, and L. Nielsen, "Biodegradable composites based on L-poly(lactide) and jute fibres," *Composites Science and Technology*, vol. 63, no. 9, pp. 1287–1296, 2003.
- [9] K. Oksman, M. Skrifvars, and J. F. Selin, "Natural fibres as reinforcement in poly(lactic acid) (PLA) composites," *Composites Science and Technology*, vol. 63, no. 9, pp. 1317–1324, 2003.
- [10] H. S. Yang, H. J. Kim, H. J. Park, B. J. Lee, and T. S. Hwang, "Effect of compatibilizing agents on rice-husk flour reinforced polypropylene composites," *Composite Structures*, vol. 77, no. 1, pp. 45–55, 2007.
- [11] M. N. Belgacem, P. Bataille, and S. Sapieha, "Effect of corona modification on the mechanical properties of polypropylene/cellulose composites," *Journal of Applied Polymer Science*, vol. 53, no. 4, pp. 379–385, 1994.
- [12] J. C. Benezet, R. B. Christensen, H. Viana, A. Bergeret, L. Ferry, and S. Borros, "Biodegradable composites from starch foam and surface plasma treated natural fiber," in *Recent Advances in Research on Biodegradable Polymers and Sustainable Composites*, vol. 1, Nova Science Publishers, New York, NY, USA, 2008.
- [13] N. E. Zafeiropoulos, C. A. Baillie, and J. M. Hodgkinson, "Engineering and characterisation of the interface in flax fibre/polypropylene composite materials. Part II. The effect of surface treatments on the interface," *Composites Part A*, vol. 33, no. 9, pp. 1185–1190, 2002.
- [14] A. K. Bledzki and J. Gassan, "Composites reinforced with cellulose based fibres," *Progress in Polymer Science*, vol. 24, no. 2, pp. 221–274, 1999.
- [15] G. Siqueira, J. Bras, and A. Dufresne, "New process of chemical grafting of cellulose nanoparticles with a long chain isocyanate," *Langmuir*, vol. 26, no. 1, pp. 402–411, 2010.
- [16] G. D. Valle, Y. Boché, P. Colonna, and B. Vergnes, "The extrusion behaviour of potato starch," *Carbohydrate Polymers*, vol. 28, no. 3, pp. 255–264, 1995.
- [17] A. Stanojlovic-Davidovic, *Matériaux biodegradables à base d'amidon expansé renforcé de fibres naturelles. Application à l'emballage alimentaire*, Ph.D. thesis, Université du Sud Toulon-Var, 2006.
- [18] J. W. Lawton, R. L. Shogren, and K. F. Tiefenbacher, "Aspen fiber addition improves the mechanical properties of baked cornstarch foams," *Industrial Crops and Products*, vol. 19, no. 1, pp. 41–48, 2004.
- [19] R. L. Shogren, J. W. Lawton, and K. F. Tiefenbacher, "Baked starch foams: Starch modifications and additives improve process parameters, structure and properties," *Industrial Crops and Products*, vol. 16, no. 1, pp. 69–79, 2002.
- [20] Z. Liu, C. S. L. Chuah, and M. G. Scanlon, "Compressive elastic modulus and its relationship to the structure of a hydrated starch foam," *Acta Materialia*, vol. 51, no. 2, pp. 365–371, 2003.
- [21] L. Averous, "Biodegradable multiphase systems based on plasticized starch: A review," *Journal of Macromolecular Science. Polymer Reviews*, vol. C44, no. 3, pp. 231–274, 2004.
- [22] D. Garlotta, "A literature review of poly(lactic acid)," *Journal of Polymers and the Environment*, vol. 9, no. 2, pp. 63–84, 2002.
- [23] R. Auras, B. Harte, and S. Selke, "An overview of polylactides as packaging materials," *Macromolecular Bioscience*, vol. 4, no. 9, pp. 835–864, 2004.
- [24] R. Mehta, V. Kumar, H. Bhunia, and S. N. Upadhyay, "Synthesis of poly(lactic acid): a review," *Journal of Macromolecular Science. Polymer Reviews*, vol. C45, no. 4, pp. 325–349, 2005.
- [25] A. Sodergard and M. Stolt, "Properties of lactic acid based polymers and their correlation with composition," *Progress in Polymer Science*, vol. 27, no. 6, pp. 1123–1163, 2002.
- [26] L. Shen, J. Haufe, and M. K. Patel, "Product overview and market projection of emerging bio-based plastics," Utrecht University 2009, www.epnoe.eu.
- [27] D. Klemmner and V. Sendjarevic, *Polymeric Foams and Foam Technology*, Hanser Garner, Munich, Germany, 1991.
- [28] M. Parikh, R. A. Gross, and S. P. McCarthy, "The influence of injection molding conditions on biodegradable polymers," *Journal of Injection Molding Technology*, vol. 2, no. 1, pp. 30–36, 1998.
- [29] C. H. Lee, K. J. Lee, H. G. Jeong, and S. W. Kim, "Growth of gas bubbles in the foam extrusion process," *Advances in Polymer Technology*, vol. 19, no. 2, pp. 97–112, 2000.
- [30] M. Saucieu, C. Nikitine, E. Rodier, and J. Fages, "Effect of supercritical carbon dioxide on polystyrene extrusion," *Journal of Supercritical Fluids*, vol. 43, no. 2, pp. 367–373, 2007.
- [31] A. Greco, A. Maffezzoli, and O. Manni, "Development of polymeric foams from recycled polyethylene and recycled gypsum," *Polymer Degradation and Stability*, vol. 90, no. 2, pp. 256–263, 2005.
- [32] S. T. Lee, L. Kareko, and J. Jun, "Study of thermoplastic PLA foam extrusion," *Journal of Cellular Plastics*, vol. 44, no. 4, pp. 293–305, 2008.
- [33] S. S. Ray and M. Okamoto, "Biodegradable polylactide and its nanocomposites: opening a new dimension for plastics and composites," *Macromolecular Rapid Communications*, vol. 24, no. 14, pp. 815–840, 2003.
- [34] Y. Ema, M. Ikeya, and M. Okamoto, "Foam processing and cellular structure of polylactide-based nanocomposites," *Polymer*, vol. 47, no. 15, pp. 5350–5359, 2006.
- [35] E. Kabir, M. C. Saha, and S. Jeelani, "Tensile and fracture behavior of polymer foams," *Materials Science and Engineering A*, vol. 429, no. 1–2, pp. 225–235, 2006.
- [36] H. R. Lin, "The structure and property relationships of commercial foamed plastics," *Polymer Testing*, vol. 16, no. 5, pp. 429–443, 1997.

- [37] M. S. Huda, L. T. Drzal, A. K. Mohanty, and M. Misra, "Effect of fiber surface-treatments on the properties of laminated biocomposites from poly(lactic acid) (PLA) and kenaf fibers," *Composites Science and Technology*, vol. 68, no. 2, pp. 424–432, 2008.
- [38] L. M. Matuana and O. Faruk, "Solid state microcellular foamed PLA and PLA/wood flour composites: morphology and property characterization," in *Proceedings of the 4th International Symposium on wood polymer composites*, Bordeaux, France, 2009.
- [39] Q. Li and L. M. Matuana, "Foam extrusion of high density polyethylene/wood-flour composites using chemical foaming agents," *Journal of Applied Polymer Science*, vol. 88, no. 14, pp. 3139–3150, 2003.
- [40] F. Mengelöglu and M. M. Laurent, "Foaming of rigid PVC/wood-flour composites through a continuous extrusion process," *Journal of Vinyl and Additive Technology*, vol. 7, no. 3, pp. 142–148, 2001.
- [41] L. M. Matuana and M. Fatih, "Manufacture of rigid PVC/wood-flour composite foams using moisture contained in wood as foaming agent," *Journal of Vinyl and Additive Technology*, vol. 8, no. 4, pp. 264–270, 2002.
- [42] S. Pilla, S. G. Kim, G. K. Auer, S. Gong, and C. B. Park, "Microcellular extrusion-foaming of polylactide with chain-extender," *Polymer Engineering and Science*, vol. 49, no. 8, pp. 1653–1660, 2009.
- [43] A. P. Mathew, K. Oksman, and M. Sain, "Mechanical properties of biodegradable composites from poly lactic acid (PLA) and microcrystalline cellulose (MCC)," *Journal of Applied Polymer Science*, vol. 97, no. 5, pp. 2014–2025, 2005.
- [44] R. Masirek, Z. Kulinski, D. Chionna, E. Piorkowska, and M. Pracella, "Composites of poly(L-lactide) with hemp fibers: morphology and thermal and mechanical properties," *Journal of Applied Polymer Science*, vol. 105, no. 1, pp. 255–268, 2007.
- [45] M. S. Huda, L. T. Drzal, A. K. Mohanty, and M. Misra, "Chopped glass and recycled newspaper as reinforcement fibers in injection molded poly(lactic acid) (PLA) composites: a comparative study," *Composites Science and Technology*, vol. 66, no. 11-12, pp. 1813–1824, 2006.



Hindawi

Submit your manuscripts at
<http://www.hindawi.com>

